



Article

Assessment of Cubic Equations of State: Machine Learning for Rich Carbon-Dioxide Systems

George Truc ¹, Nejat Rahmanian ^{1,*} and Mahboubeh Pishnamazi ²

¹ Chemical Engineering Department, Faculty of Engineering & Informatics, University of Bradford, Bradford BD7 1DP, UK; GeorgeTruc@ChemEng.uk

² Department of Chemical Sciences, Bernal Institute, University of Limerick, Limerick V94 T9PX, Ireland; Seyedeh.pishnamazi@ul.ie

* Correspondence: n.rahmanian@bradford.ac.uk

Abstract: Carbon capture and storage (CCS) has attracted renewed interest in the re-evaluation of the equations of state (EoS) for the prediction of thermodynamic properties. This study also evaluates EoS for Peng–Robinson (PR) and Soave–Redlich–Kwong (SRK) and their capability to predict the thermodynamic properties of CO₂-rich mixtures. The investigation was carried out using machine learning such as an artificial neural network (ANN) and a classified learner. A lower average absolute relative deviation (AARD) of 7.46% was obtained for the PR in comparison with SRK (AARD = 15.0%) for three components system of CO₂ with N₂ and CH₄. Moreover, it was found to be 13.5% for PR and 19.50% for SRK in the five components' (CO₂ with N₂, CH₄, Ar, and O₂) case. In addition, applying machine learning provided promise and valuable insight to deal with engineering problems. The implementation of machine learning in conjunction with EoS led to getting lower predictive AARD in contrast to EoS. An of AARD 2.81% was achieved for the three components and 12.2% for the respective five components mixture.



Citation: Truc, G.; Rahmanian, N.; Pishnamazi, M. Assessment of Cubic Equations of State: Machine Learning for Rich Carbon-Dioxide Systems. *Sustainability* **2021**, *13*, 2527. <https://doi.org/10.3390/su13052527>

Academic Editor: Farooq Sher

Received: 24 January 2021

Accepted: 20 February 2021

Published: 26 February 2021

Publisher's Note: MDPI stays neutral with regard to jurisdictional claims in published maps and institutional affiliations.



Copyright: © 2021 by the authors. Licensee MDPI, Basel, Switzerland. This article is an open access article distributed under the terms and conditions of the Creative Commons Attribution (CC BY) license (<https://creativecommons.org/licenses/by/4.0/>).

Keywords: equation of state (EoS); carbon capture systems (CCS); machine learning; fluid package selection

1. Introduction

The increased global awareness of the effect of CO₂ on the climate has renewed the interest in carbon capture and storage (CCS) technologies for the reduction of CO₂ emissions relative to historic emissions; these innovative technologies aim to achieve a lower relative rise in global mean temperature (GMT) long-term [1]. Though the accurate prediction of the thermodynamic properties of CO₂-rich mixtures is critical in terms of design calculations for the selectivity, costing, and safety of operations, improper property prediction will have an adverse effect on a project's economic feasibility in regards to overdesign or lack thereof [2,3].

1.1. A Brief Insight into Equation of State and Machine Learning

There are a vast number of equations of state (EoS) used for the prediction of thermodynamic properties of gas mixtures. These EoS are used in a fluid package within software such as Aspen HYSYS to predict fundamental properties such as density, heat capacity, viscosity, etc. [4]. Also, it is highly important to combine the existing EoS with other methods to improve the reliability and accuracy of predicting thermodynamic properties. It is because using EoS in the design calculations in software packages such as AspenONE, without access to autonomous property prediction programmes such as NIST Thermo Data Engine [5], is not sufficiently accurate. Machine learning itself can be used to predict property data, however, current works are limited to species within fractional components X, Y, etc. Combined with EoS principles, it can be used to predict mixtures' thermody-

dynamic properties more accurately and at a wider range using artificial variables such as pseudo-reduced variables within the data pre-processing [6].

1.2. Rise of Machine Learning in Science

With the emergence of Industry 4.0, some of its key pillars such as machine learning have been implemented into industries and a range of academic fields to provide a novel solution to Big Data problems [7]. Machine learning is a statistical-based model for computer systems to perform tasks such as data prediction and classification from the analysis of a set of inputs without an explicit set predefined logical model such as conventional empirical correlation equations [7]. Machine learning builds a model through the use of a training dataset where a set of variables would be used to predict the desired output [8]. There are two main types of learning: supervised and unsupervised, both of which have an assortment of applications. Supervised learning is a novel solution for the current empirical models such as those used in cubic EoS through the specification of their respective input parameters such as temperature, pressure, and composition to train the system to learn the relationship through non-linear modeling and may provide a solution within minutes whereas more accurate models will require significantly longer depending on the complexity of the model. An innovative solution may also be to use unsupervised learning, where only the input and output are given, where the predicted model will categorize data as various classes (such as solid, liquid, or vapor).

There has been little work done on the combination of machine learning with artificial variables for the prediction of thermodynamic properties, where recent works such as work presented by Nikkholgh (2009) [6] considered the use of reduced variables, however, did not consider the use of Bayesian regularization backpropagation and the combination of the variables from cubic EoS such as the attraction and repulsion factors [6]. This is because of the lack of powerful computing in artificial intelligence (AI) [7]. Also, despite the adaptation of first-principles-based models to problems, there is still a lack of capability to model problems such as diagnosis, safety analysis, and materials design [9]. Therefore, it is imperative to focus on machine-learning-based technologies such as AI. AI technologies such as Deep Learning and ANN have the capability and should be further investigated to make the method mature within chemical engineering [9].

The machine learning tools used in this work made use of the toolbox found in MATLAB software [10] that has both supervised and unsupervised learning functionality for the data prediction with a full list of modeling techniques. In this work, the supervised learning model was performed for the classification and regression of fluid properties. The main feature of this work employs the use and development of an ANN, which makes use of the Neural Network Fitting app within the machine learning toolbox for the prediction of density; whereas for the prediction of phase behavior, classified learning was used.

1.3. Aspen Fluid Package Selection

This article aims to cover the evaluation of the cubic EoS of the Carlson (1996) physical property selection method for Aspen, which suggests the use of Peng–Robinson, Redlich–Kwong–Soave, and Lee–Kesler–Plocker for their reliability in carbon-rich mixtures prediction [11]. Although it seems that PR is the preferred equation for gas mixtures due to its low critical Z value, new mixing rules like Predictive-SRK and UMR have changed this perception [12]. The EoS is known for its empirical nature, and there is a need to constantly evaluate the correct mixture behavior. Thus, it is highly useful to review the fundamental principles behind cubic EoS for their application in machine learning algorithms.

2. Materials and Methods

2.1. Cubic Equation of State

Cubic equations of state are a popular practice used for property predictions of chemical processes due to their simplicity and the assimilation into Maxwell constructions for thermodynamic departure predictions [13]. Van der Waals was the first to successfully

find the PVT behavior in gas and liquid states by including a repulsive and attraction term [14]. The underlying principle of the Van der Waals' equation is the description of phase behavior through dimensionless reduced variables (a , b , and c constants) relating to reduced fluid properties: T_r , P_r , and V_r which is defined by the Equation (1):

$$T_r = \frac{T}{T_c}; P_r = \frac{P}{P_c}; V_r = \frac{V}{V_c} \quad (1)$$

These reduced variables yield a universal reduced equation, though this principle is valid for substances that present similar PVT behavior in terms of reduced variables [15]. The theorem of corresponding states for fluid phases is expressed by a compressibility factor (Z) (Equation (2)), which may be used in the ideal gas formulae to define real fluid properties:

$$Z = \frac{P \times V_m}{R \times T} \quad (2)$$

The nature of cubic EoS, being of cubic nature, allows for three possible roots, where T_r being smaller than 1 can enter the vapor-liquid equilibrium regime, though as the reduced temperature is decreased further, minima and maxima are present (for the turning point) in the equation of state shown in where three real roots are present. It has been observed that the low-temperature results in a metastable fluid, this phenomenon is known as "stretched liquid" and causes negative absolute pressure. However, this is not further explored in this work [16]. As a result of the abovementioned Corresponding States Theorem, the root for the basis of prediction for all cubic EoS has empirical correlations to the critical compressibility of a set of mixtures.

$$Z_c = \frac{P_c \times V_{m_c}}{R \times T_c} \approx Constant \quad (3)$$

Van Der Waals acknowledges that substances behave alike at the same reduced states, that being said, at their respective reduced state the properties of these substances are alike, which is known as the corresponding states principle. Hence, the primary purpose of the use of corresponding states is for the cubic empirical model [17]:

$$P = \frac{R \times T}{V_m - b} - \frac{a}{V_m(V_m + b) + c(V_m - b)} \quad (4)$$

The tabulation of the cubic equation of state in Table 1 is found in the literature where Van der Waals, RK, SRK, PR, Harmens–Knapp, and Schmidt–Wenzel EoS were obtained from [13]; Patel–Teja [18], and the modified Nasrifar Moshfeghian EoS [19].

Table 1. Cubic Equations of State Variations [13,18,19].

Cubic Equation	a	b	c	Simplified Equation
Van der Waals	a	0	0	$P = \frac{R \times T}{V_m - b} - \frac{a}{V_m^2}$
Redlich and Kwong	$\frac{a}{\sqrt{T_r}}$	b	0	$P = \frac{R \times T}{V_m - b} - \frac{a}{(\sqrt{T_r}) V_m (V_m + b)}$
Soave Modified Redlich Kwong	$a \times \alpha$	b	0	$P = \frac{R \times T}{V_m - b} - \frac{a \times \alpha}{V_m (V_m + b)}$
Peng Robinson	$a \times \alpha$	b	B	$P = \frac{R \times T}{V_m - b} - \frac{a \times \alpha}{V_m (V_m + b) + b (V_m - b)}$
Harmens-Knapp				$P = \frac{R \times T}{V_m - b} - \frac{a(T)}{V_m^2 + V_m \times b \times c + b^2 \times (c - 1)}$
Schmidt-Wenzel				$P = \frac{R \times T}{V_m - b} - \frac{a(T)}{V_m^2 + V_m \times b \times (1 + 3\omega) + b^2 \times 3\omega^2}$
Patel-Teja				$P = \frac{R \times T}{V_m - b} - \frac{a(T)}{V_m^2 + V_m(b + c) - b \times c}$
Modified Nasrifar Moshfeghian				$P = \frac{R \times T}{V_m - b(\varnothing)} - \frac{a_c \times a(\varnothing)}{V_m^2 + 2 \times b(\varnothing) \times V_m - 2 \times b(\varnothing)^2}$

The parameters for the EoS have an approximate physical meaning, where a is the attraction force between the molecules, b is related to the repulsion and the effective molecule size [20]. The a and b parameters used in this work as presented in Table 2 [16]. The table lists the original works where the Soave-modified Redlich–Kwong alpha function is modified for hydrogen-containing systems due to the conventional extension. This is unable to accurately predict the K values of hydrogen, which may be required in syngas processing [21].

Table 2. Cubic equations of interest parameters [16].

Cubic Equation	a	B	α
Redlich and Kwong	$0.42748 \times \frac{R^2 \times T_c^5}{P_c}$	$0.08664 \times \frac{R \times T_c}{P_c}$	
Soave Modified Redlich Kwong	$0.42748 \times \frac{R^2 \times T_c^5}{P_c}$	$0.08664 \times \frac{R \times T_c}{P_c}$	$[1 + (0.48508 + 1.55171 \times \omega - 0.15613 \times \omega^2) \times (1 - T_r^{0.5})]^2$
Peng Robinson	$0.45724 \times \frac{R^2 \times T_c^2}{P_c}$	$0.0778 \times \frac{R \times T_c}{P_c}$	$[1 + (0.37464 + 1.54226 \times \omega - 0.26992 \times \omega^2) \times (1 - T_r^{0.5})]$

EoS extension to mixtures requires the use of mixing rules to calculate pseudo-reduced properties; the rules applied for mixtures may be as basic as linear mixing, assuming no activity between mixture species. An improvement is an extension to mixtures through the use of Van der Waals mixing for pseudo-reduced attraction and repulsion parameters through interaction parameters. There are two popular mixing rules including linear (Equations (5)–(7)) and Van Der Waals (Equations (6)–(8)) mixing rules [13].

$$a_{mix} = \sum_{i=1}^N X_i \times a_i \quad (5)$$

$$b_{mix} = \sum_{i=1}^N X_i \times b_i \quad (6)$$

$$c_{mix} = \sum_{i=1}^N X_i \times c_i \quad (7)$$

$$a_{mix} = \sum_{i=1}^N \sum_{j=1}^N X_i \times X_j \times (a_i \times a_j)^{0.5} \times (1 - k_{ij}) \quad (8)$$

In the current study, in contrast to the semi-empirical correlation, the binary interaction coefficients (k_{ij}) were extracted from the Aspen HYSYS database for Peng–Robinson and Soave–Redlich–Kwong to solve Equation (8). The binary interaction coefficients for Peng Robinson and Soave Redlich Kwong are provided in Tables 3 and 4.

Table 3. Peng Robinson Binary interaction parameters [19].

	Carbon Dioxide	Nitrogen	Methane	Argon	Oxygen
Carbon Dioxide	0	-2.00×10^{-2}	0.1	0	9.75×10^{-2}
Nitrogen	-2.00×10^{-2}	0	3.60×10^{-2}	0	-1.20×10^{-2}
Methane	0.1	3.60×10^{-2}	0	2.30×10^{-2}	0
Argon	0	0	2.30×10^{-2}	0	1.04×10^{-2}
Oxygen	9.75×10^{-2}	-1.20×10^{-2}	0	1.04×10^{-2}	0

Table 4. SRK Binary interaction parameters [19].

	Carbon Dioxide	Nitrogen	Methane	Argon	Oxygen
Carbon Dioxide	0	-1.71×10^{-2}	9.56×10^{-2}	0	9.75×10^{-2}
Nitrogen	-1.71×10^{-2}	0	3.12×10^{-2}	-2.00×10^{-3}	-1.40×10^{-2}
Methane	9.56×10^{-2}	3.12×10^{-2}	0	3.90×10^{-2}	0
Argon	0	-2.00×10^{-3}	3.90×10^{-2}	0	1.60×10^{-2}
Oxygen	9.75×10^{-2}	-1.40×10^{-2}	0	1.60×10^{-2}	0

For the evaluation of EoS and the development of the Artificial Neural Network model, pure component properties, and the properties of a binary mixture such as density and viscosity data were obtained from the literature. For the prediction of binary mixture components, the obtaining of their respective pure component physical properties was undertaken using NIST databanks for properties such as critical pressure, temperature, volume, relative molecular mass, and acentric factor. The pure component properties are given in Table 5. For the development of a single fluid property prediction, the work was done by [21] by measuring densities and thermodynamic properties for three CO₂-rich mixtures.

Table 5. Physical properties for pure substances [21].

Component	RMM	Critical Properties			Acentric Factor (Unitless)	Standard Ideal Gas Formation of	
		Pressure, MPa	Temperature, K	Volume, m ³ /mol		Enthalpy (kJ/mol)	Gibbs Energy (kJ/mol)
Carbon Dioxide	44.010	7.38	304.18	9.4120×10^{-5}	0.228	−393.51	−394.39
Nitrogen	28.013	3.40	40.55	8.9081×10^{-5}	0.040	0	0
Methane	16.043	4.60	190.56	9.8630×10^{-5}	0.011	−74.8	−50.8
Argon	39.948	4.87	150.8	7.4303×10^{-5}	0	0	0
Oxygen	31.998	5.05	154.6	7.9997×10^{-5}	0.022	0	0

2.2. Models Development

2.2.1. EoS Phase Property Prediction Methodology for EoS Evaluation

Firstly, the evaluation of EoS models including Redlich–Kwong, the Soave-modified Redlich–Kwong, and Peng–Robinson was performed for the prediction of carbon-dioxide-rich mixtures for their use in simulation software. The compressibility of the CO₂ mixtures is computed through a three-step process: pseudo-critical properties calculation, mixture attraction-repulsion coefficient calculation, and solving of general EoS. The first step utilizes the linear mixing rule to predict the critical temperature and pressure of the mixture. The second step extends the use of the selected EoS to mixtures; the prediction of cubic equation parameters *a*, *b*, and α employs Van der Waals mixing using the VW_{mix} script, where the binary interaction coefficients are inputted from the Aspen HYSYS database, whereas for the three components in the Peng–Robinson EoS, the works by [21] are incorporated for the improved modeling of the VLE behavior. The third step uses the MATLAB symbolic toolbox. The compressibility is solved numerically for V_m of the general EoS (in Equation (4)) by using the appropriate variables calculated using Van der Waals mixing for their respective equations: RK, SRK, and PR.

Using the “if” condition to compute the real roots, we classify whether they are in a single-phase region or classify as liquid or vapor by specifying minimum and maximum roots respectively. The molar density may be computed by the reciprocal of the molar volume. The outputs of this function are the compressibility and molar density of the liquid, gas, and single-phase systems.

2.2.2. Machine Learning

The development of machine learning tools for property prediction made use of Knime Analytics and MATLAB, the computation of phase behavior using Weka posed several limitations which in turn led to it not being included in this study due to the inability to have a systematic approach to prediction through a set architecture.

For the prediction of properties of CO₂ mixtures, the logic presented in Figure 1 shows the stages undertaken for the optimization and development of each generation of model envisaged through MATLAB. The sequence of events that lead to the advancement and success in a model lay within the pre-processing data stage, where the manipulation of input data (in this article, the experimental data from literature [22–24]) is to extract desired data points and remove irrelevant data, where this data is then used in the calculation of parameters; these techniques for data manipulation are altered where needed to improve predictive accuracy over the preceding model. The manipulated data is then collected for training in the neural network model alongside the specified selected number of layers, neurons per layer, and training algorithm; the trained model is then computed for the AARD.

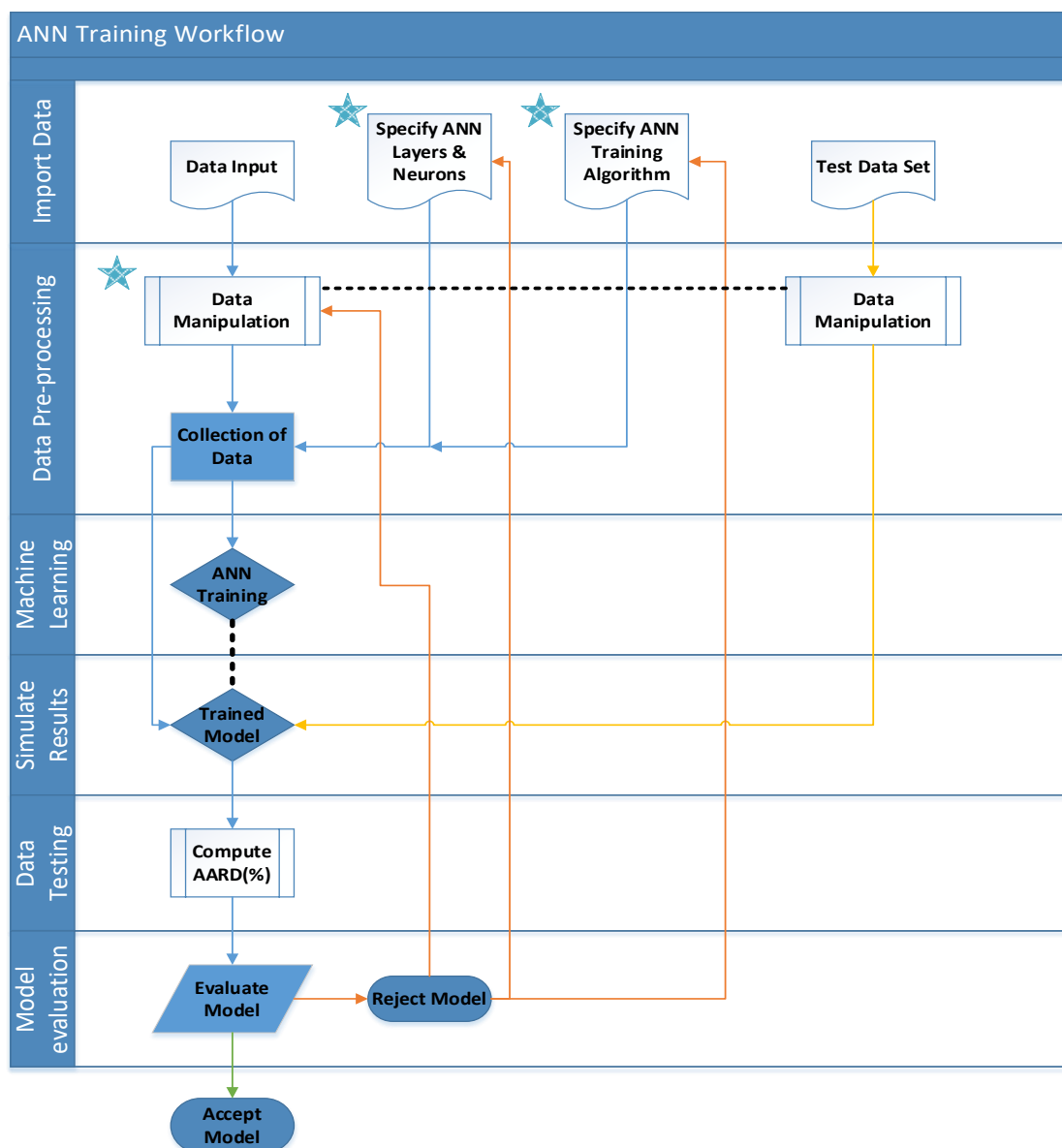


Figure 1. Artificial neural network training workflow logic.

Within the “Evaluation” stage when the AARD is computed for the neural network model, the model is contrasted against its predecessors for its accuracy and reliability, if it deviates this too much, the alteration of the pre-processing parameters (marked by blue stars below) such as data manipulation method, neuron-layers, and layers-per-neuron is changed to achieve the lowest AARD.

The approach to achieving the improved models with the enhanced data pre-processing technique is presented in the following sections. It is important to note that each model may require to be re-run, this is due to many solutions available from each unique model owed to the random seed of assigned weights in the initialization of the neural network model, which are then optimized around.

Generation 1 and 2—Knime Analytics

The first and second-generation for property prediction in this work made use of Knime Analytics for the prediction of the density for a single binary mixture at a temperature and pressure range of 273–423 K and 0.95–126.46 MPa, respectively. Generation 1 (Figure 2) comprised of the prediction of density by training the MLP using temperature, pressure, and composition, however, it was found that around the phase boundary prediction issues arose.

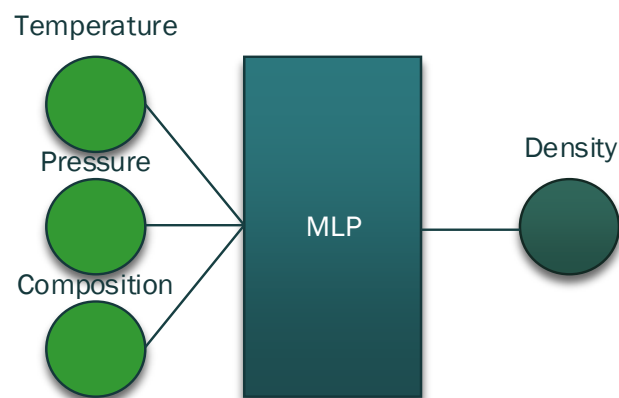


Figure 2. Generation 1 for density prediction using MLP.

The phase prediction error is reduced in Generation 2 (Figure 3) where data input is partitioned by phase into their respective categories. This method required more time to compute the data due to the increase in the number of MLP for each phase and offers no solution to property prediction.

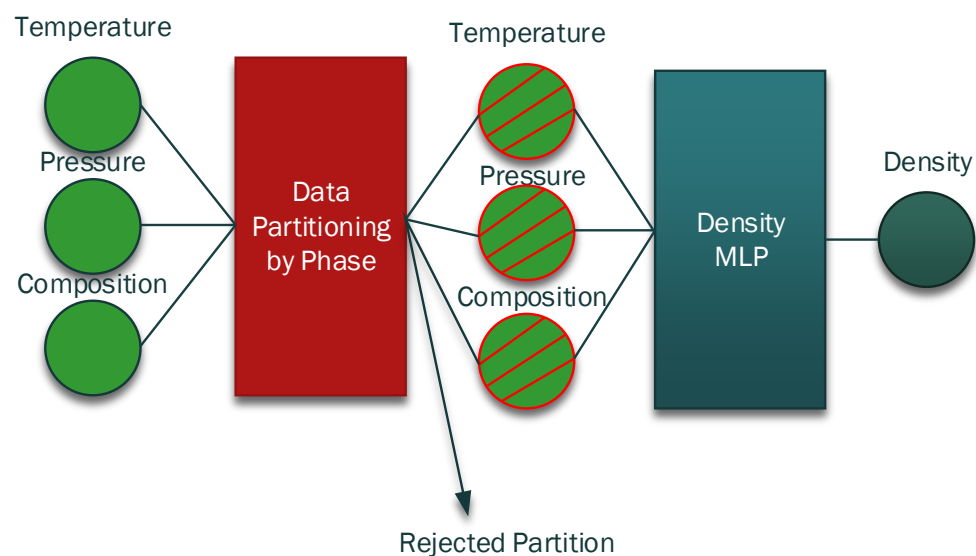


Figure 3. Generation 2 for prediction of density through Split Data.

Generation 3 and 4—Initial MATLAB Models for Predicting Density and Viscosity

The third-generation model developed is aimed at predicting viscosity along with density (Figure 4), however, an improvement was made by using the predicted density as an additional input using an ANN in series (see Figure 5).

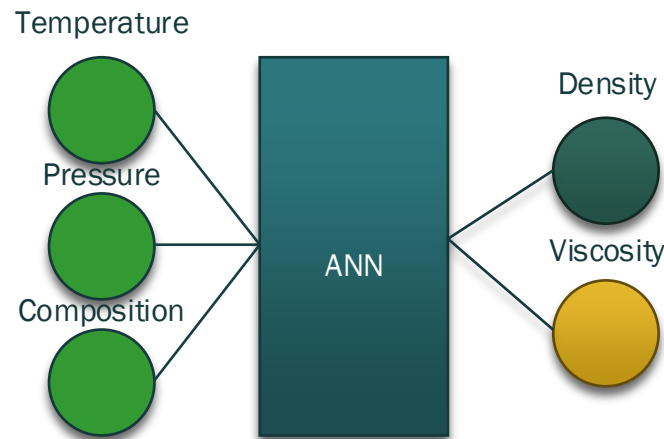


Figure 4. Gen 3 density and viscosity prediction ANN workflow.

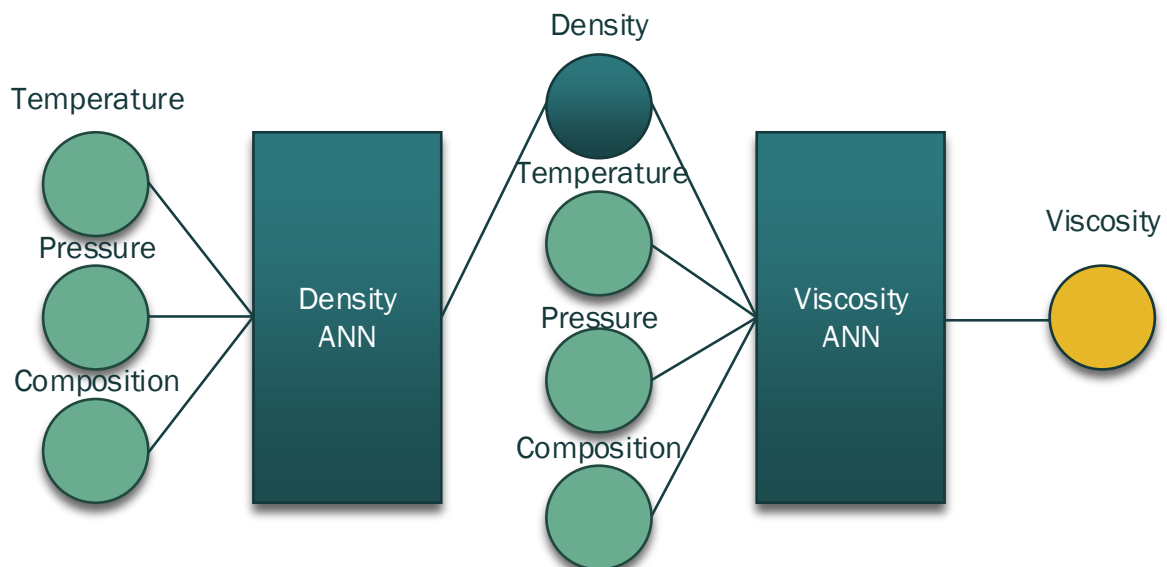


Figure 5. Generation 4 improved viscosity prediction with density ANN workflow.

Generation 3 and 4—Initial MATLAB Models for Predicting Density and Viscosity

Generation 5 (Figure 6) is aimed at improving upon Generation 2, with the prediction of density close to the phase boundary. The prediction of phase uses the MATLAB classification learner through support vector machines (SVM) for the separation of two classes of data through a hyperplane, or a soft margin when necessary. The training set used for training the classifier module defined the phases: gas as “1”, liquid as “2”, and supercritical as “3”; exporting this model for the prediction phase from the input temperature and pressure for pre-processing and then training the ANN to predict density (see Figure 6).

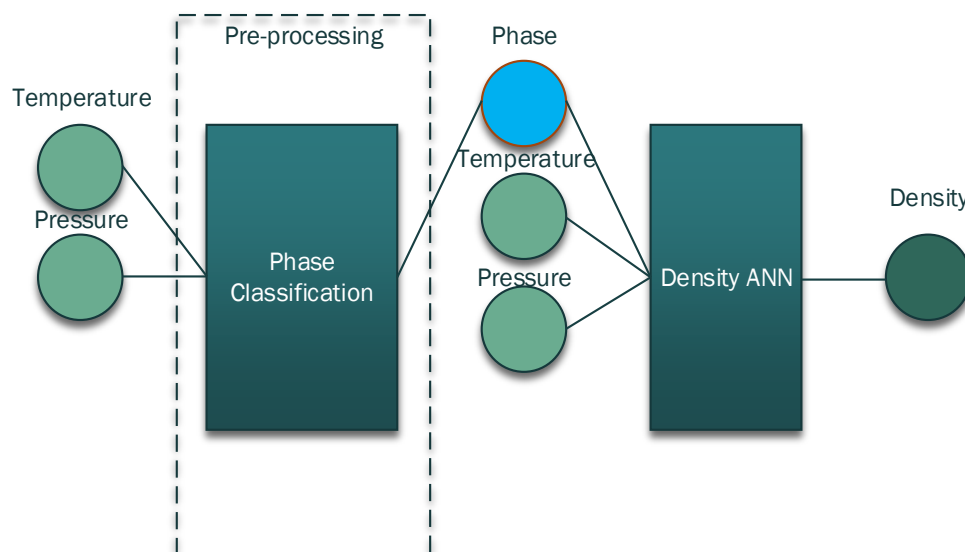


Figure 6. Generation 5 Density prediction ANN with phase classification workflow.

Generation 6—Association with Equation of State Parameters

With both the ANN and cubic EoS models working and ANN showing higher accuracy in contrast to Peng–Robinson and SRK; for the improvement on existing works for the property prediction of pure CO₂, the extension of mixtures was undertaken. A new ANN schema for property prediction was envisioned (Figure 7) using functions of:

- Pseudo-reduced temperature and pressure.
- Peng–Robinson attraction and repulsion parameters.
- Pseudo-critical compressibility (though not incorporated in the final model).

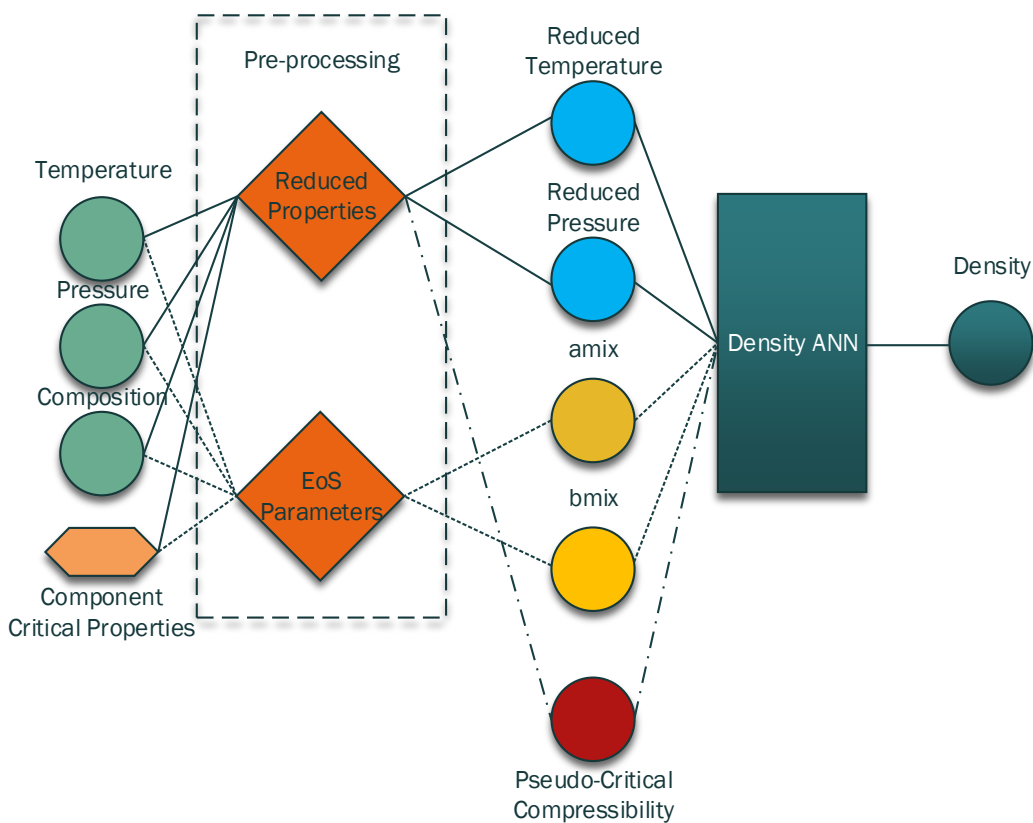


Figure 7. Generation 6 workflow of density prediction through various pre-ANN processing techniques.

3. Results and Discussion

3.1. Generation 1 and 2 Multi-Layered Perceptron (Knime Analytics)

Knime Analytics was used for the prediction of density. Table 6 (temperature between 6.71 K and 77.94 K) and Table 7 (temperature between 273.4 K and 323.4 K) show the input, output, and the deviation of the predicted densities from the experimental value. AARDs (%) of 22.27% and 5.95% were obtained for temperatures between 6.71 K and 77.94 K and temperatures between 273.4 K and 323.4 K, respectively. There are two higher absolute relative deviations (ARDs) in Table 6, which make the average higher for the temperature between 6.71 K and 77.94 K. Generally, this method is quite appropriate for the prediction of a mixture density, especially at a higher temperature.

Table 6. Generation 2 results of Knime Analytics MLP density prediction of the test set for mixture 1 (6.71 K to 77.94 K) [22].

Phase	Input		Output		Relative Deviation (%)	ARD (%)
	Temperature (K)	Pressure (MPa)	Density (kg/m ³)			
			Experimental	Calculated		
L	6.71	88.8	385.2	820.4	112.98	112.98
L	51.73	107.36	1071.4	1082.5	1.04	1.04
G	1.81	3.76	59.2	56.5	−4.58	4.58
L	6.36	81.08	239.8	758.2	216.13	216.13
L	22.57	95.63	943.5	943.8	0.04	0.04
L	36.41	100.46	997.5	1008.3	1.08	1.08
L	54.13	105.21	1049.7	1061.6	1.13	1.13
L	105.09	114.13	1145.2	1141.2	−0.35	0.35
L	50.12	99.96	996.4	1010.0	1.36	1.36
L	126.33	114.56	1142.9	1149.7	0.59	0.59
G	2.19	3.74	46.3	39.0	−15.59	15.59
SC	15.88	64.24	732.5	723.9	−1.18	1.18
SC	54.07	94.15	942.9	942.9	0.00	0.00
SC	77.97	100.87	1012.0	1012.1	0.01	0.01
SC	26.16	56.85	612.0	611.8	−0.02	0.02
SC	77.94	90.08	907.3	909.2	0.21	0.21
				Min	−15.59	Average
				Max	216.13	22.27

Table 7. Generation 2 results of Knime Analytics MLP density prediction of the test set for mixture 1 (273.4 K to 323.4 K) [22].

Phase	Input		Output		Relative Deviation (%)	ARD (%)
	Temperature (K)	Pressure (MPa)	Density (kg/m ³)			
			Experimental	Calculated		
L	273.4	6.71	888	820.4	−7.61	7.61
L	273.4	51.73	1073.6	1082.5	0.83	0.83
G	283.3	1.81	37.6	56.5	50.15	50.15
L	283.3	6.36	810.8	758.2	−6.49	6.49
L	283.3	22.57	956.3	943.8	−1.30	1.30
L	283.3	36.41	1004.6	1008.3	0.37	0.37
L	283.3	54.13	1052.1	1061.6	0.90	0.90
L	283.3	105.09	1141.3	1141.2	−0.01	0.01
L	298.4	50.12	999.6	1010.0	1.04	1.04
L	298.4	126.33	1145.6	1149.7	0.36	0.36
G	323.4	2.19	37.4	39.0	4.40	4.40

Table 7. Cont.

Input			Output			
Phase	Temperature (K)	Pressure (MPa)	Density (kg/m ³)		Relative Deviation (%)	ARD (%)
			Experimental	Calculated		
SC	323.4	15.88	642.4	723.9	12.69	12.69
SC	323.4	54.07	941.5	942.9	0.14	0.14
SC	323.4	77.97	1008.7	1012.1	0.34	0.34
SC	373.5	26.16	568.5	611.8	7.63	7.63
SC	373.5	77.94	900.8	909.2	0.94	0.94
				Min	−7.61	Average
				Max	50.15	5.95

3.2. Generation 3 and 4 Neural Network Prediction of Density and Viscosity (MATLAB)

Neural network was used for the prediction of viscosity of a single-phase binary mixture. Table 8 shows an improved prediction of viscosity with lower minimum, maximum, and AARD.

Table 8. Summary of results for ANN prediction of single-phase viscosity for CO₂ and Squalene [18].

	Prediction of Viscosity		
	Density	Gen 3 (No Density)	Gen 4 (With Density)
Min Deviation (%)	−1.014	−37.670	−8.469
Max Deviation (%)	1.144	34.959	5.807
AARD (%)	0.230	4.121	1.130

3.3. Generation 3 and 4 Neural Network Prediction of Density and Viscosity (MATLAB)

For the prediction of phase through SVM, investigating the accuracy of each method for the number of folds (where data is divided into portions using 1 for test validation and the rest for training repeating through each fold and taking an average error). Generally, it was found that cubic is more accurate than the other ones (Table 9).

Table 9. MATLAB classified Learner accuracy with phase prediction.

Number of Folds	SVM Accuracy (%)					
	Linear	Quadratic	Cubic	Fine Gaussian	Medium Gaussian	Coarse Gaussian
1 (No Validation)	96.80	100.00	100.00	98.40	88.90	76.20
2	88.90	96.80	98.40	90.50	85.70	74.60
4	95.20	93.70	98.40	93.70	85.70	77.80
6	88.90	90.50	93.70	88.90	74.60	69.80
8	96.80	96.80	95.20	95.20	82.50	76.20
10	96.80	95.20	98.40	96.80	85.70	76.20
15	95.20	93.70	93.70	93.70	82.50	74.60
20	96.80	96.80	95.20	96.80	84.10	77.80
30	96.80	95.20	96.80	95.20	85.70	74.60
40	96.80	95.20	95.20	96.80	84.10	76.20
50	96.80	95.20	96.80	96.80	84.10	76.20

Note: Colour coded for each fold where green is most accurate in set and red being least accurate.

3.4. Comparison of 3 and 5 Component Binary Mixtures for EoS and Generation 6 ANN with the Association of EoS (MATLAB)

For the computation of Generation 6 ANN, two layers with six neurons each with the Bayesian regularization backpropagation algorithm for the reduction in overfitting of data and consistency in results were used. The following subsections present a graphical

comparison of compressibility for the computed EoS and ANN against the literature data for pure CO₂, CO₂ in a binary mixture with N₂ and CH₄. As can be seen, ANN has a lower AARD (%) of 2.81. After that, the PR is more accurate than the RK and SRK (see Table 10).

Table 10. Absolute deviation for EoS and ANN for three components from the MATLAB model.

	RK	SRK	PR	ANN
Maximum ARD (%)	98.77	290.09	271.83	65.70
AARD (%)	52.25	14.98	7.46	2.81

Using the full dataset of CO₂ with N₂, CH₄, Ar, and O₂, as there is no available data (for the selection of the number of components) for the binary interaction coefficients for the self-consistent equations, the Van der Waals mixing rule was computed using Aspen interaction parameters [20]. The outcome of this led to ANN being significantly more accurate than the earlier components (Table 11).

Table 11. Absolute deviation for EoS and ANN for five components from MATLAB model.

	RK	SRK	PR	ANN
Maximum ARD (%)	569.89	659.02	638.98	553.57
AARD (%)	79.77	19.39	13.29	12.24

Generally, in terms of machine learning tools, MATLAB is a better choice for model development than using Knime Analytics due to the increased customization of ANN setup, monitoring of performance, and integration into the property prediction framework. In the case of Weka, though the software is not used to generate results, the analytics package has the opportunity to export the design of neuron layers' respective bias and weight to incorporate the ANN into MATLAB and other code-based mathematical software. The major issue that arose with using MATLAB, which is not presented in Knime Analytics, is the associating of a "seed" to the neural network. This allows for a continually changing framework of the network through different seed converses of the neural network, however, this may be avoided by storing the state of the random number generator before the initialization of the network.

The complete generations of neural network models developed all have merit to property prediction, Generation 3 and 4 for viscosity prediction show a suitable degree of accuracy for prediction, the benefit of using density as an input though has provided a significant reduction in maximum error. In Generation 5, to combat the issue arising phase change, classifying the phase as an independent variable through the Classification Learner app, the best classification method using support vector machines is its cubic variant, this is expected as the phase characterization as a function of temperature and pressure is of cubic behavior.

The use of pseudo-critical properties such as reduced pressure, temperature, and EoS parameters in the Generation 6 model for ANN predictions is able to predict compressibility as a single output because of this, vapor liquid equilibria may not be solved in this version and will have to be undertaken in future works, though the main objective was to achieve an ANN that is able to predict compressibility more accurately than the other methods. However, with the five-component binary mixtures, like with EoS, the predictive accuracy decreased.

In this work, Bayesian regularization backpropagation had the lowest AARD, followed by Levenberg–Marquardt backpropagation. However, in published literature Bayesian regularization has not been considered.

3.5. Comparison of 3 and 5 Component Binary Mixtures for EoS and Generation 6 ANN with the Association of EoS (MATLAB)

The major issue arising from the modeling of data is the overfitting of the training data. Even with the use of the Bayesian regularization backpropagation training function, the data still overfitted the training data. This is shown in Figure 8 where the algorithm attempts to find the optimal solution, however, after 600 iterations the MSE of the training set increases significantly with near to no improvement of the actual training set. Though in cases where the number of neurons is lower, such as Figure 9, the optimum solution is found and is not limited by the maximum epoch to prevent overfitting. The current limitation of this work is the prediction of mixture critical properties, as such, a more accurate method for predicting mixture pseudo-critical properties is desired for improving prediction through a better mixing rule for pseudo-properties calculation, where currently linear mixing is used. The optimal ANN setup was found using the three-component mixture. It was obtained that the optimal number of neurons per layer is between two and eight, however, with too many neurons, the AARD deteriorates, overfitting the data and not being able to converge to find the optimal setup. Though the optimal number of layers showed that two neuron layers are the ideal setup for this case; however, it is unable to find optimum weight and bias values to achieve an appropriate fit for the data, unlike with one layer. In this work, it was found that the Bayesian regularization backpropagation has the lowest AARD. Figure 8 shows AARD% as a function of the number of neurons. From Figure 10, increasing from one layer to two layers led to the reduction of AARD% significantly. It may be because the outputs of the ANN model are not a linear function of the input. Moreover, a considerable change in AARD% was not seen with the increase of the number of layers from two to three. Therefore, two layers were selected as the optimal value.

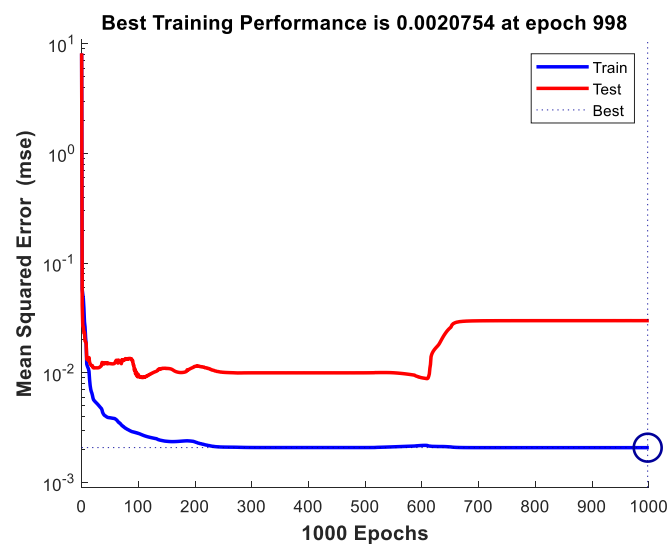


Figure 8. Training Performance for 100 Neuron ANN.

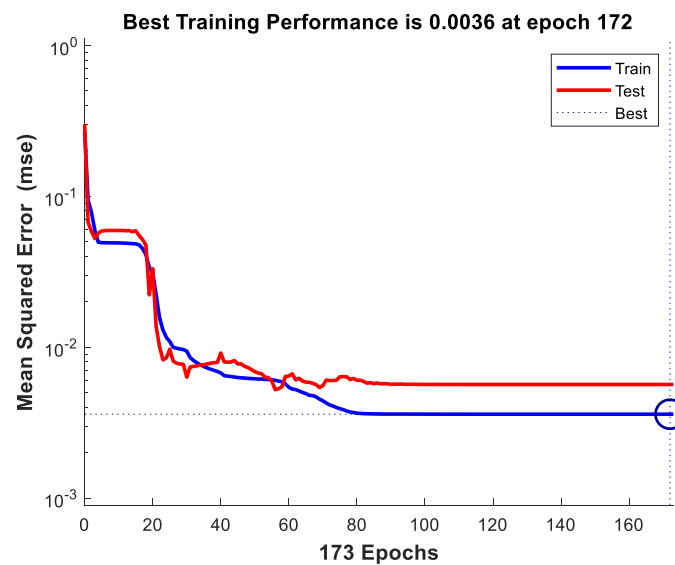


Figure 9. Training Performance for 10 Neuron ANN.

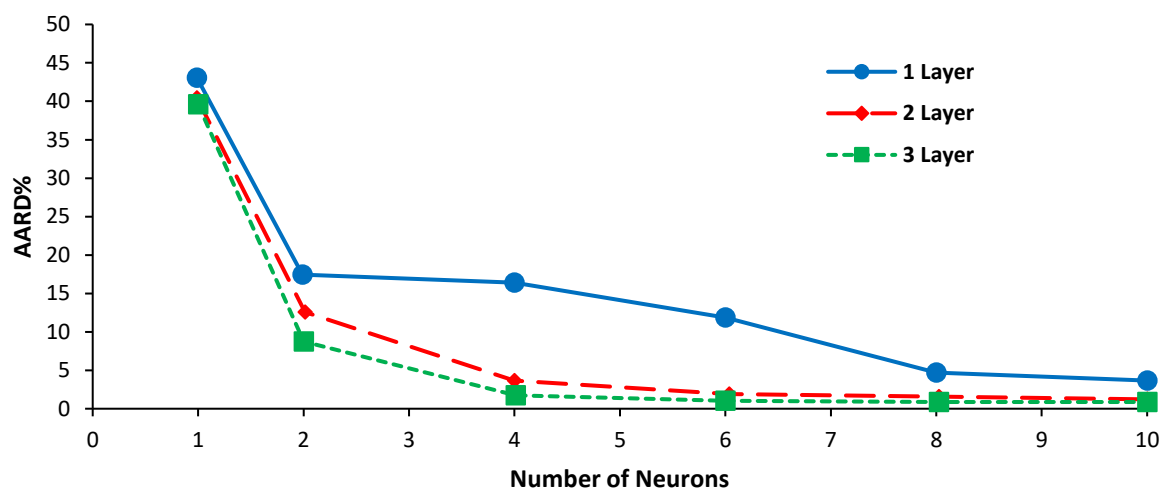


Figure 10. Optimal number of neurons and layers AARD (Training).

3.6. Compressibility Factor

The gas compressibility factor or Z-factor is one of the most vital parameters in the industries such as chemical and petroleum. It should be pointed out that there is a direct relationship between the Z-factor and the density of a gas stream, its flow rate as well as isothermal compressibility [25]. It is challenging to obtain accurate Z-factor values for gas streams because of the fact that mostly there are other gases in the CO₂-rich mixture gas and also the system is non-ideal [25]. It is common to use simple empirical correlations for the prediction of the Z-factor, however, the results are usually not accurate and there are calculation convergence difficulties [25]. A combination of different methods can be used to improve the compressibility factor prediction. The work done by Gaganis [26] combined the truncated regularized kernel ridge regression (TR-KRR) algorithm with a simple linear-quadratic interpolation scheme for estimation of the Z-factor. The maximum absolute relative prediction error is around the critical point was obtained around 2%. In the present study, the combination of machine learning with EoS was used for the prediction of the compressibility factor of pure CO₂ and CO₂-rich mixtures. The compressibility factor as a function of reduced pressure for the pure CO₂ models for SRK and Peng–Robinson EoS and ANN at three different temperatures were shown in Figure 11. The results showed

high accuracy when dealing with the prediction of compressibility factor, however, this was due to the more ideal state of the system. It was assumed that the system is pure CO₂.

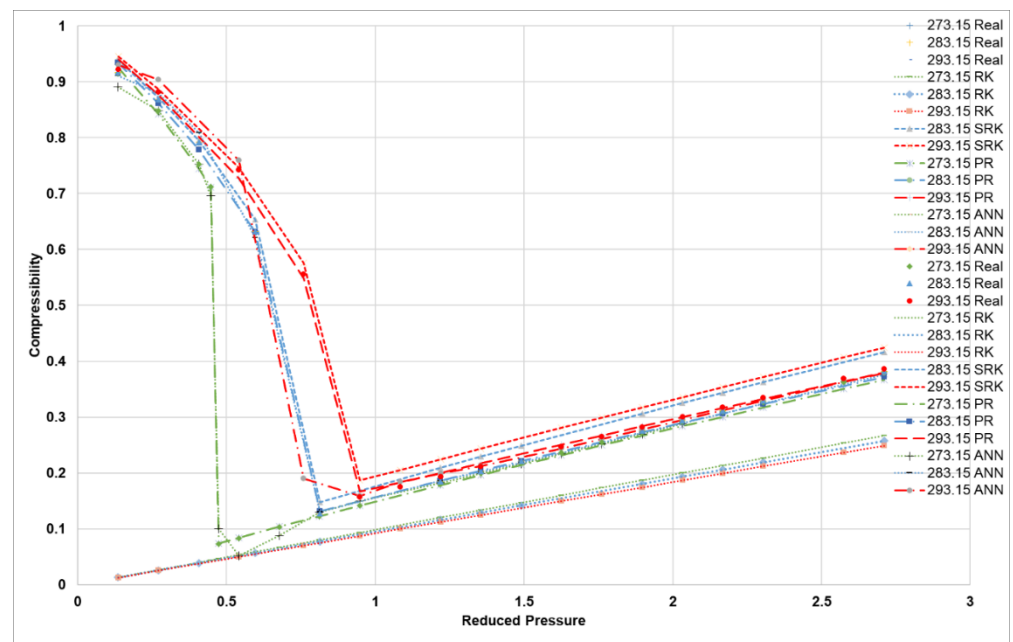


Figure 11. Pure CO₂ compressibility chart for all temperatures.

Compressibility as a function of reduced pressure for a binary mixture containing N₂ (mole fraction = 0.0442) at three different temperatures is shown in Figure 12. For a binary mixture with the low mole fraction of nitrogen (N₂ mole fraction = 0.0442). As it can be seen the SRK, PR, and ANN can predict the compressibility factor relatively accurately at the points far from the critical points. However, the accuracy of the ANN model is higher at the points around critical points. It can be seen as higher deviations for all three EoS at the critical points.

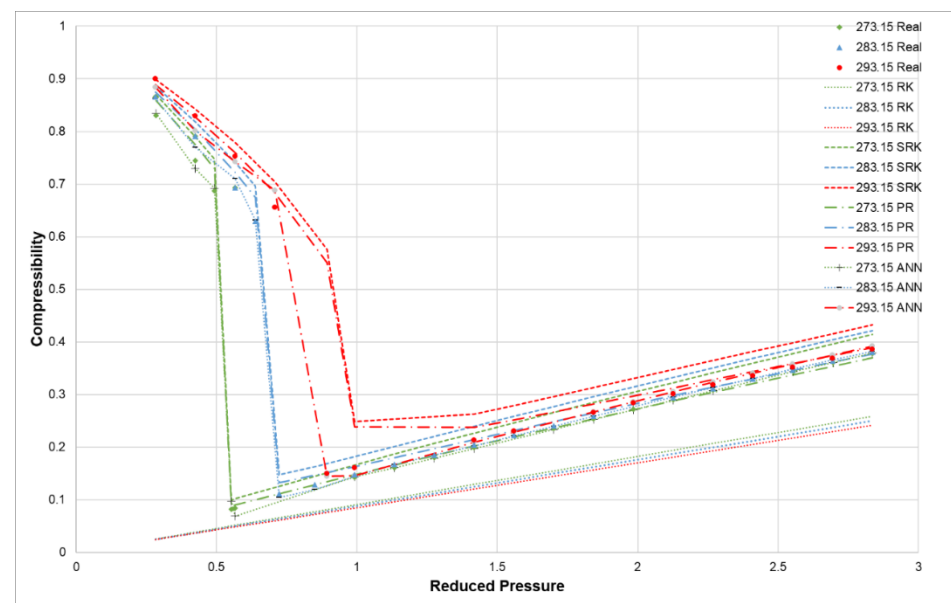


Figure 12. CO₂ and N₂ binary mixture compressibility chart (x_{CO_2} : 0.9558).

The nitrogen content in the gas mixture was increased to evaluate the effect of the higher N₂ content of the gas mixture. The compressibility factor as a function of reduced

pressure for a binary mixture containing N_2 (mole fraction = 0.0442 and 0.1442) at three different temperatures is shown in Figures 13 and 14. It was found that there is a lower deviation from experimental data at a lower temperature in the presence of a higher N_2 mole fraction (0.1442) for all three EoS and ANN was higher in the gas mixture. Interestingly, it obtained fairly accurate results even for the RK EoS at lower temperature and higher N_2 content in comparison with pure CO_2 (Figure 11) and lower N_2 content (Figure 12) but significant deviation was found for the RK EoS at temperatures of 283 K and 293 K. The deviation from experimental data was increased for the SRK and PR EoS, when temperature increased to 283 K and 293 K, at the points around the critical point. However, there was good agreement between the ANN model values and the experimental data for all three temperatures.

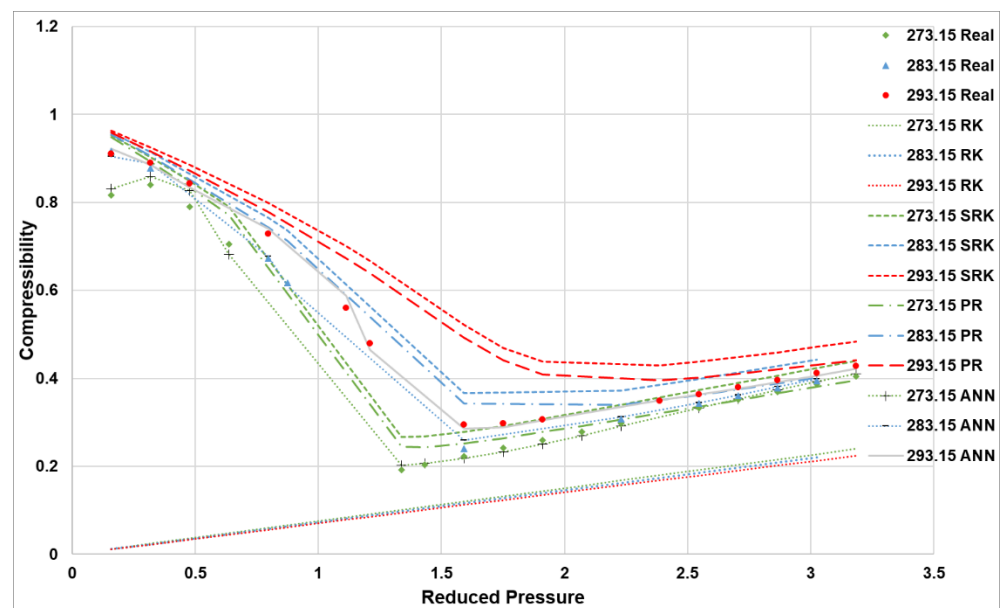


Figure 13. CO_2 and N_2 binary mixture compressibility chart (x_{CO_2} : 0.8512).

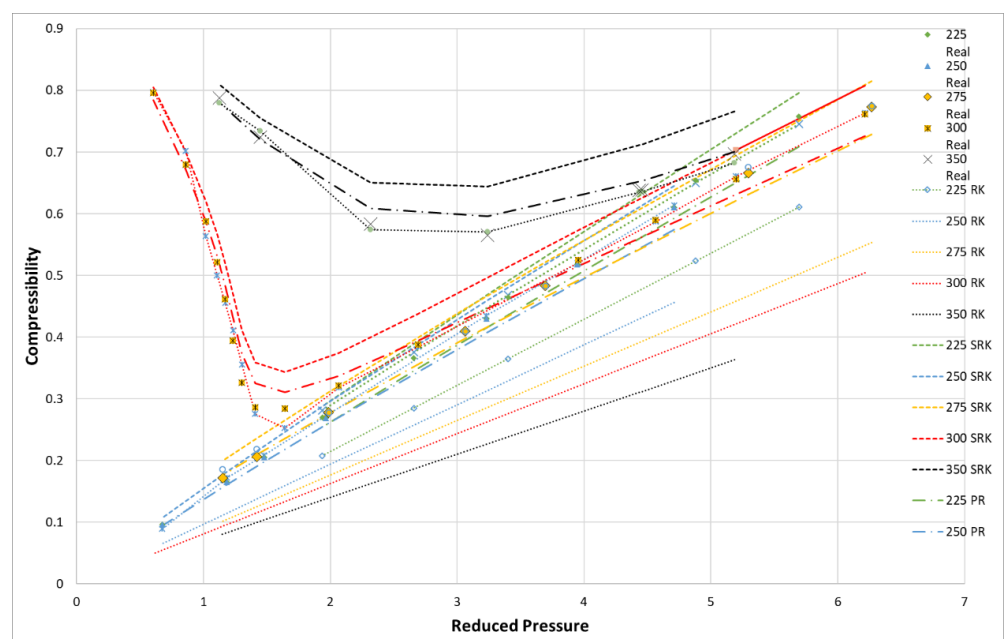


Figure 14. CO_2 and N_2 binary mixture compressibility chart (x_{CO_2} : 0.9558).

4. Conclusions

The objective of this work was to select an appropriate model for the prediction of thermodynamic properties for CO₂-rich mixtures. This is clearly of high value to the simulation for the future of process design in CCS and adsorption kinetic in gas-well application. Out of the evaluated EoS that is used in Aspen HYSYS, Peng–Robinson more accurately represents CO₂ mixtures. Though there are more accurate EoS developed in the literature, these works are not yet available to incorporate into process simulation using Aspen HYSYS.

The applicability of machine learning techniques applied from Big Data analytics to a broader range of problem-solving capabilities for chemical engineering such as empirical formulation has been successfully considered in this work and may further be used for process control. Prospects of this work aim to incorporate machine learning into process simulations software, where literature or experimental data may be used to accurately describe fluid properties for process design using a pre-set model that is capable of defining a fluid accurately without the need for empirical formulation or choosing a “close enough” approach to using a selection of preset fluid packages.

The importance of data manipulation has been successfully addressed in this article to provide a basis for manipulation of input data to enhance predictive accuracy by extending the desired outputs from being mol fractional inputs of individual components to being a function of pseudo-critical properties. This development may lead to an improved universal model to predict a complex range of mixtures thermodynamic property from their fundamental particle interactions and other underlying mixture interactions not yet explored in this article.

Having explored a range of training algorithms in this work, it has been found that using Bayesian regularization backpropagation has not been previously considered in the published literature [6], which is surprising due to its better classification of data with lower AARD in contrast to conventional lowest AARD, being Levenberg–Marquardt backpropagation. Perhaps this should be considered more throughout the development of ANN for predicting thermodynamic properties in future works.

Author Contributions: Conceptualization, G.T. and N.R.; Data curation, G.T.; Formal analysis, G.T.; Investigation, G.T.; Methodology, G.T.; Project administration, N.R.; Software, G.T.; Supervision, N.R.; Visualization, G.T.; Writing—original draft, G.T. and M.P.; Writing—review and editing, G.T., N.R., and M.P. All authors have read and agreed to the published version of the manuscript.

Funding: This research received no external funding.

Institutional Review Board Statement: Not applicable.

Informed Consent Statement: Not applicable.

Data Availability Statement: The data presented in this study are openly available in references [23–25].

Conflicts of Interest: The authors declare no conflict of interest.

References

1. Anderson, C.; Beer, P.; Broad, R.; Brown, A.; Bui, M.; Darton, R.; Dixon, P.; Fennell, P.; Green, M.; Hackett, L.; et al. A Chemical Engineering Perspective on the Challenges and Opportunities of Delivering Carbon Capture and Storage at Commercial Scale. 2018. Available online: <https://www.icheme.org/media/1401/ccs-report-2018.pdf> (accessed on 25 August 2019).
2. Boomsma, C.; Ter Mors, E.; Jack, C.; Broecks, K.; Buzoianu, C.; Cismaru, D.M.; Peuchen, R.; Piek, P.; Schumann, D.; Shackley, S.; et al. Community compensation in the context of Carbon Capture and Storage: Current debates and practices. *Int. J. Greenh. Gas Control* **2020**, *101*, 103128. [CrossRef]
3. Tan, W.-L.; Ahmad, A.; Leo, C.; Lam, S.S. A critical review to bridge the gaps between carbon capture, storage and use of CaCO₃. *J. CO₂ Util.* **2020**, *42*, 101333. [CrossRef]
4. National Institute of Standards and Technology. Search for Species Data by Chemical. In *NIST Chemistry WebBook*; National Institute of Standards and Technology: Gaithersburg, MA, USA, 2018.
5. Bismukhametov, T.; Jäschke, J. Combining machine learning and process engineering physics towards enhanced accuracy and explainability of data-driven models. *Comput. Chem. Eng.* **2020**, *138*, 106834. [CrossRef]

6. Nikkholgh, M.R.; Moghadassi, A.R.; Parvizian, F. *A New Approach for Estimating Compressibility Factor of Natural Gas Based on Artificial Neural Network*; International Chemical Engineering Congress & Exhibition: Kish, Iran, 2009; pp. 1–6.
7. Venkatasubramanian, V. The promise of artificial intelligence in chemical engineering: Is it here, finally? *AIChE J.* **2019**, *65*, 466–478. [[CrossRef](#)]
8. Sizochenko, N.; Syzochenko, M.; Fjodorova, N.; Rasulev, B.; Leszczynski, J. Evaluating genotoxicity of metal oxide nanoparticles: Application of advanced supervised and unsupervised machine learning techniques. *Ecotoxicol. Environ. Saf.* **2019**, *185*, 109733. [[CrossRef](#)] [[PubMed](#)]
9. Al-Jabery, K.; Obafemi-Ajayi, T.; Olbricht, G.; Wunsch, D. *View on ScienceDirect Computational Learning Approaches to Data Analytics in Biomedical Applications*, 1st ed.; Academic Press: Cambridge, MA, USA, 2019; Volume 1.
10. Carlson, E.C. Don't Gamble with Physical Properties for Simulations. *Chem. Eng. Prog.* **1996**, *92*, 35–46.
11. Kontogeorgis, G.M.; Coutsikos, P. Thirty Years with EoS/GEModels—What Have We Learned? *Ind. Eng. Chem. Res.* **2012**, *51*, 4119–4142. [[CrossRef](#)]
12. Adachi, Y.; Sugie, H.; Lu, B.C.-Y. Evaluation of cubic equation of state. *J. Chem. Eng. Jpn.* **1984**, *17*, 624–631. [[CrossRef](#)]
13. Harmens, A.; Knapp, H. Three-Parameter Cubic Equation of State for Normal Substances. *Ind. Eng. Chem. Fundam.* **1980**, *19*, 291–294. [[CrossRef](#)]
14. Onken, U.; Fischer, K.; Rarey, J. Estimation of Physical Properties. In *Ullmann's Encyclopedia of Industrial Chemistry*; Wiley: Hoboken, NJ, USA, 2000.
15. Imre, A.; Martínás, K.; Rebelo, L.P.N. Thermodynamics of Negative Pressures in Liquids. *J. Non-Equilibrium Thermodyn.* **1998**, *23*, 351–375. [[CrossRef](#)]
16. Patel, N.C. The Calculation of Thermodynamic Properties and Phase Equilibria Using a New Cubic Equation of State. 1980. Available online: https://repository.lboro.ac.uk/articles/thesis/The_calculation_of_thermodynamic_properties_and_phase_equilibria_using_a_new_cubic_equation_of_state/9237890 (accessed on 10 August 2019).
17. Forero, G.L.A.; Velásquez, J.J.A. A modified Patel–Teja cubic equation of state: Part I—Generalized model for gases and hydrocarbons. *Fluid Phase Equilibria* **2013**, *342*, 8–22. [[CrossRef](#)]
18. Salehpour, A.R.; Nasrifar, K. Predicting the Liquid Density of Gas Condensates and LNG Mixtures from Equations of State. *J. Algorithms Comput.* **2013**, *42*, 257–268. Available online: https://jac.ut.ac.ir/article_7751.html. (accessed on 27 August 2019).
19. Graboski, M.S.; Daubert, T.E. A Modified Soave Equation of State for Phase Equilibrium Calculations. 3. Systems Containing Hydrogen. *Ind. Eng. Chem. Process. Des. Dev.* **1979**, *18*, 300–306. [[CrossRef](#)]
20. AspenTech. *Aspen HYSYS*; AspenTech: Bedford, MA, USA, 2019.
21. Fateen, S.-E.K.; Khalil, M.M.; Elnabawy, A.O. Semi-empirical correlation for binary interaction parameters of the Peng–Robinson equation of state with the van der Waals mixing rules for the prediction of high-pressure vapor–liquid equilibrium. *J. Adv. Res.* **2013**, *4*, 137–145. [[CrossRef](#)] [[PubMed](#)]
22. Mohagheghian, E.; Zafarian-Rigaki, H.; Motamedi-Ghahfarrokhi, Y.; Hemmati-Sarapardeh, A. Using an artificial neural network to predict carbon dioxide compressibility factor at high pressure and temperature. *Korean J. Chem. Eng.* **2015**, *32*, 2087–2096. [[CrossRef](#)]
23. Nazeri, M.; Chapoy, A.; Burgass, R.; Tohidi, B. Measured densities and derived thermodynamic properties of CO₂-rich mixtures in gas, liquid and supercritical phases from 273 K to 423 K and pressures up to 126 MPa. *J. Chem. Thermodyn.* **2017**, *111*, 157–172. [[CrossRef](#)]
24. Hwang, C.-A.; Iglesias-Silva, G.A.; Holste, J.C.; Hall, K.R.; Gammon, B.E.; Marsh, K.N. Densities of Carbon Dioxide + Methane Mixtures from 225 K to 350 K at Pressures up to 35 MPa. *J. Chem. Eng. Data* **1997**, *42*, 897–899. [[CrossRef](#)]
25. Mazzocoli, M.; Bosio, B.; Arato, E. Pressure–Density–Temperature Measurements of Binary Mixtures Rich in CO₂ for Pipeline Transportation in the CCS Process. *J. Chem. Eng. Data* **2012**, *57*, 2774–2783. [[CrossRef](#)]
26. Gaganis, V.; Homouz, D.; Maalouf, M.; Khoury, N.; Polychronopoulou, K. An Efficient Method to Predict Compressibility Factor of Natural Gas Streams. *Energies* **2019**, *12*, 2577. [[CrossRef](#)]